PHYSICAL REVIEW B VOLUME 27, NUMBER 2 15 JANUARY 1983

Correlated random walk in lattices: Tracer diffusion at general concentration

R. A. Tahir-Kheli
Department of Physics, Temple University, Philadelphia, Pennsylvania 19122

R. J. Elliott
Department of Theoretical Physics, University of Oxford, 1 Keble Road, Oxford, England
(Received 14 July 1982)

A problem of considerable physical interest, wherein a tracer of arbitrary species diffuses against a dynamic background of double occupancy avoiding classical particles of concentration x hopping on regular lattices, is studied. The theory is exact to the leading order in vacancy concentration, $v=1-x$, and to two leading orders in x. Moreover, in the intermediate concentration, it incorporates all the dominant fluctuations from the mean field. Results are worked out for a variety of quantities of interest, such as the tracer diffusion coefficient, the dynamic response, as well as the generalized diffusional mass operator for all the Bravais cubic lattices. New insights are obtained regarding the rapid variation of the response and the mass operator near the Brillouin-zone edge as a function of the vacancy concentration when $v \ll 1$. Inversion of the K-dependent characteristics of these quantities, not noticed heretofore, is reported and analyzed.

I. INTRODUCTION

Under appropriate conditions ionic motion in superionic conductors,[1] tracer atom diffusion in hot solids via the vacancy mechanism,[2] and diffusion of hydrogen in various metal hydrides[3] can all be described in terms of simple hopping motion of classical particles. The model generally assumes that the hopping occurs only between lattice sites separated by a specified distance, that it is instantaneous (i.e., that the particle spends most of its time localized at lattice sites and very little, if any, in the delocalized state pertaining to its transit between them) and, above all, that hopping is a stochastic process, independent of the past history of the particle. Such hopping motion is, nevertheless, correlated since a particle cannot hop onto a site which at that particular instant is already occupied. Similarly, despite the stochastic nature of the hopping process itself, there is an important memory correlation which arises through the interplay of the self-avoidance characteristic of all the hopping particles and the stochasticity of the allowed hops. A graphic representation of such space-time memory effects is a simple process in which after a recently completed hop, for example, from site i to j, site i is seen to retain a larger than average probability that it is still empty and thus available for a return hop.

In view of such memory effects the so-called "random-walk" motion of self-avoiding particles is not at all random. Rather, the space-time correlation has the effect of coupling the motion of particles separated over macroscopic space and time distances. A well-known consequence of this is the occurrence of the correlation factor in the expression for the tracer diffusion which is substantially different from unity.[4,5] A less well-known, but even more dramatic effect of these correlations is found in the low-frequency wave-vector—dependent diffusional response (or, equivalently, in the mass operator) at the zone boundary.[6]

Procedures for the calculation, and measurement, of tracer diffusion coefficients[4,5] in the small vacancy limit are now well established, and the corresponding results are readily obtained for a fairly general set of situations, including the case of vacancy-assisted diffusion of a tracer with an arbitrary jump rate[2] (in units of the vacancy-particle interchange rate of the host particles). Unfortunately, these theoretical procedures are applicable only to the evaluation of the classical diffusion coefficient. Accordingly, they provide only very limited information about the incoherent, self-correlation response function relating to the limit of vanishingly small frequencies and wave vectors. In view of the refinements in Mössbauer spectroscopy, improvements in the NMR techniques, availability of spin-echo spectrometers, and above all the development of high-resolution, high-flux slow neutron spectroscopy, interest in the line shape of the diffusional response over a wide spectrum of frequency and wave vectors has sharpened.

Indeed, interest in the evaluation of the full response dates back to the early 1950s, when Torrey[7]

presented a calculation based on phenomenological considerations. More succinct quantitative attempts were later made by Singwi and Sjölander,[8] who used a mean-field decoupling of the dynamical equations, and Chudley and Elliott,[9] who described the relevant correlations in the limit of an empty lattice.

A sophisticated theoretical analysis of the frequency and wave-vector–dependent response was undertaken by Fedders and Sankey (FS) a few years ago. In an important series of papers[10–15] they put forward diagrammatic procedures for calculating dominant contributions to frequency moments of the response function. While neither the moments nor the response function constructed from them were made available[16] in any explicit form, results for the tracer diffusion coefficient were presented which are accurate to three digits in both of the nontrivial limits (i.e., when $v\to 0$ and also in the limit $x\to 0$). Moreover, FS predictions agree to within a couple of percent with numerical simulation estimates for the self-diffusion coefficient over the whole concentration range.[17,18]

Despite the commanding stature of the FS work in this field, its applicability is restricted to the case of self-diffusion: namely, to the case where the hopping characteristics of the tracer and the host atoms are identical. This is a serious limitation in view of the fact that suitable tracers are often different from the host particles.[2] Moreover, interest in incoherent neutron scattering from metal hydrides with hydrogen tracers diffusing against a background of hopping deuterium atoms[19–21] has heightened the need for a more general analysis. In particular, results are needed for systems with hopping rates which, rather than being identical to that of the background particles, are arbitrary. Moreover, in addition to the $\vec{K}\to 0$, $\omega\to 0$ results for the tracer diffusion coefficients, a readily accessible description of the general $\vec{K}$- and ω-dependent characteristics of the response is needed for arbitrary concentrations.

To this end, we present here a treatment for the arbitrary tracer hopping rate J^0. The background particle hopping rate is J. In Sec. II, after a brief description of the model, the relevant equations of motion of the correlation functions are given. The nature of the truncation is discussed to bring out the physical motivation behind the approximation. The solution and some analytical results are presented in Sec. III. Section IV deals with numerical results for the response function and the mass operator. This paper concludes with a discussion of the results.

II. EQUATIONS OF MOTION

As is usual in this field,[10–23] we make a number of simplifying assumptions. Particle hops are restricted to occur between neighboring lattice positions. Moreover, the mechanics of the hop are simplified to a picture where the particle is assumed to spend essentially all of its time localized on lattice sites. Accordingly, a relatively insignificant time is taken for completing any hop that it undertakes (during which the particle is in transit between the relevant two sites).

These assumptions are implicit in the following rate equations referring to the stochastic occupancy variables of the tracer as well as those of the hopping host particles,

$$\frac{dp_i}{dt}=-\sum_j J^0_{ij}[p_i(1-n_j)-p_j(1-n_i)]\ , \tag{2.1}$$

$$\frac{dn_i}{dt}=-\sum_j J_{ij}[n_i(1-p_j)-n_j(1-p_i)]\ . \tag{2.2}$$

Here p is the stochastic occupancy variable referring to the tracer and n is the corresponding variable relating to the host atoms. Accordingly, if at time t a lattice site i is occupied by the tracer, than $p_i(t)=1$; otherwise, $p_i(t)=0$. Similarly, $n_i(t)=1$, or 0, according to whether or not one of the host atoms is present at site i at time t. The hopping rate parameters, because of the restriction of the hopping range mentioned earlier, have the following property:

$$\mathscr{K}_{ij}=\mathscr{K}_{ji}=\begin{cases}\mathscr{K} & \text{if } i \text{ and } j\\ & \text{are nearest neighbors}\\ 0 & \text{otherwise}\end{cases} \tag{2.3}$$

$(\mathscr{K}\equiv J^0 \text{ or } J)$.

Care has to be exercised in handling any rate equations relating to more than one particle, since the chain rule for computing time derivatives does not apply in its usual form. This aspect of the time derivatives of stochastic occupancy variables has been emphasized by Richards.[22] Moreover, some of its formal consequences have been noted in the FS work.[10–15]

We define the tracer occupancy Green's function,

$$G_{gg'}(t)=-2\pi i\Theta(t)\langle p_g(t)p_{g'}(0)\rangle\ , \tag{2.4a}$$

and its frequency Fourier transform,

$$G_{gg'}\equiv\langle\langle p_g;p_{g'}\rangle\rangle=\frac{1}{2\pi}\int_{-\infty}^{+\infty}G_{gg'}(t)\exp(i\omega t)dt\ , \tag{2.4b}$$

where $\Theta(t)$ is the usual Heaviside step function

$$\Theta(t)=\begin{cases}+1 & \text{for } t>0\\ 0 & \text{otherwise,}\end{cases} \tag{2.4c}$$

and the single angular brackets denote a statistical

average. The rate equation (2.1) now readily leads to the relationship

$$\omega G_{gg'}=\delta_{gg'}-iv\sum_j J^0_{gj}(G_{gg'}-G_{jg'}) +i\sum_j J^0_{gj}(G^{(2)}_{gj;g'}-G^{(2)}_{jg;g'}) . \tag{2.5}$$

Here v denotes the vacancy concentration in the hopping host lattice. Assuming x to be the atomic concentration in this lattice, i.e.,

$$x=1-v=\langle n_j\rangle , \tag{2.6}$$

the two-particle propagators $G^{(2)}$ occurring in Eq. (2.6) are defined as follows:

$$G^{(2)}_{lj;g'}=\langle\langle p_l u_j;p_{g'}\rangle\rangle , \tag{2.7}$$

where

$$u_j=n_j-x,\langle u_j\rangle=0 . \tag{2.8}$$

Within simple mean-field approximations[8] (MFA), such propagators $G^{(2)}$ are assumed to be negligible. These approximations are useful only to the extent that dynamic fluctuations of the stochastic variable u_j are insignificant. A useful, qualitative estimate for the range of validity of the unembellished MFA can be obtained as follows: The neglect of fluctuations in u_j would be more acceptable, the smaller its variance σ. In other words, errors inherent in the MFA mass operator may be expected to be of order $\sigma\omega^0_K$, where

$$\sigma=\langle u_j^2\rangle=xv , \tag{2.9}$$

and ω^0_K is the unblocked, tracer diffusion mode frequency, i.e.,

$$\omega^0_K=J^0z(1-\gamma_K) , \tag{2.10}$$

$$\gamma_K=\frac{1}{z}\sum_{\vec\delta}\exp(i\vec k\cdot\vec\delta) . \tag{2.11}$$

(Here $\vec\delta$ represents one of the z nearest-neighbor lattice vectors.)

Thus we see that in a Fourier-transformed representation (with respect to the inverse lattice space) the contribution of the first set of terms on the right-hand side of Eq. (2.5) is $v\omega^0_K G_K$, whereas the fluctuations (i.e., the scattering terms represented by $G^{(2)}$) are proportional to $xv\omega^0_K G_K$. Accordingly, the neglect of fluctuations would be acceptable if their relative size, with respect to the retained MFA terms, is small. This happens only when $x\to 0$. Since the fluctuations get larger as x increases, the $v\to 0$ limit represents the worst possible regime for the application of the unembellished MFA.

In order to improve upon the MFA in a systematic and meaningful fashion, a careful accounting of the scattering terms in Eq. (2.5) is needed. To this purpose, we examine below the equation of motion of $G^{(2)}$,

$$\omega G^{(2)}_{lj;g'}=-\delta_{lj}x\omega G_{lg'}-ix(zJ^0v+zJ)\delta_{lj}G_{lg'}+ix(vJ^0_{lj}+J_{lj})G_{lg'}+ixJ^0_{lj}G^{(2)}_{jl;g'} +iG^{(2)}_{lj;g'}[(v-x)J^0_{lj}+J_{lj}-z(J^0v+J)]+i\left[\sum_i J^0_{li}G^{(2)}_{ij;g'}v+\sum_i J_{ji}G^{(2)}_{li;g'}\right](1-\delta_{lj})+\mathscr{R}_{lj;g'} . \tag{2.12}$$

In the above, the remainder $\mathscr{R}$ is linearly proportional to three-body scattering terms of the general form

$$G^{(3)}_{1,23;g'}\equiv\langle\langle p_1u_2u_3;p'_g\rangle\rangle , \tag{2.13}$$

where sites 1, 2, and 3 are *all different*. Consequently, the neglect of the remainder $\mathscr{R}$ contributes errors of the order

$$\langle u_1^2u_2^2\rangle\omega^0_K\underset{1\neq 2}{\sim}x^2v^2\omega^0_K \tag{2.14}$$

to the mass operator of our basic Green's function G_K. This statement is rigorously correct in both the $x\to 0$ and the $v\to 0$ limits, and is qualitatively valid in this form in the intermediate concentration regime. Thus, in order to obtain the mass operator for the basic Green's function G which is exact to the linear order in v and to orders x^0 and x for small x, Eqs. (2.5) and (2.12) have to be solved simultaneously, neglecting the third-order fluctuation terms embodied in the remainder $\mathscr{R}$. Such a solution is presented below.

III. THE SECOND-ORDER SOLUTION

It is convenient to replace spatial dependence with one involving inverse lattice wave vectors. This entails using Fourier transformation,

$$G_{gg'}=\frac{1}{N}\sum_K G_K\exp[i\vec K\cdot(\vec g-\vec g\,')] , \tag{3.1a}$$

$$G^{(2)}_{lj;g'}=\left[\frac{1}{N}\right]^2 \times\sum_{K_1}\sum_{K_2}G^{(2)}_{K_1,K_2}\exp[i\vec K_1\cdot(\vec l-\vec g\,') +i\vec K_2\cdot(\vec j-\vec g\,')] , \tag{3.1b}$$

$$\delta_{gg'}=\frac{1}{N}\sum_K \exp[i\vec{K}\cdot(\vec{g}-\vec{g}')] . \tag{3.1c}$$

The equation of motion, (2.5), is now represented in the form

$$(\omega+iv\omega_K^0)G_K=1+iJ^0\sum_\delta[1-\exp(i\vec{k}\cdot\vec{\delta})]f_k(\vec{\delta}) . \tag{3.2}$$

For arbitrary $\vec{K}$ and ω, there are a total of z different $f_K(\vec{\delta})$'s.

It is convenient to define the function

$$f_K(\vec{r})=\frac{1}{N}\sum_\lambda \exp(-i\vec{\lambda}\cdot\vec{r})G^{(2)}_{K-\lambda,\lambda}$$
$$=\frac{1}{N}\sum_l\sum_{g'}\langle\langle p_l u_{l-r};p_{g'}\rangle\rangle \times\exp[-i\vec{k}\cdot(\vec{l}-\vec{g}')] . \tag{3.3}$$

It represents the propagation of the tagged particle and a vacancy held at a fixed relative distance $\vec{r}$, and propagating together through the crystal with $\vec{K}$. It satisfies the Fourier-transformed second-order equation of motion (2.12),

$$\omega f_K(\vec{r})=-xG_K\left[\delta(\vec{r})[\omega+iz(J^0v+J)]-\sum_{\delta'}\delta(r-\delta')i(J^0v+J)\right]$$
$$-i\delta(\vec{r})\sum_{\delta'}[J^0v\exp(-i\vec{K}\cdot\vec{\delta}')+J]f_K(\vec{r}-\vec{\delta}')$$
$$+i\sum_{\delta'}[J^0v\exp(-i\vec{K}\cdot\vec{\delta}')+J]f_K(\vec{r}-\vec{\delta}')-iz(J^0v+J)f_K(\vec{r})$$
$$+i\sum_{\delta'}\delta(\vec{r}-\vec{\delta}')\{[J^0(v-x)+J]f_K(\vec{r})+xJ^0\exp(-i\vec{K}\cdot\vec{\delta}')f_K(-\vec{r})\} . \tag{3.4}$$

If the interaction terms which occur for $\vec{r}=0$ or $\vec{\delta}$ are neglected, the free propagation of the particle-vacancy pair is given by

$$P_K(\vec{r},\vec{r}')=\frac{1}{N}\sum_\lambda\frac{\exp[-i\vec{\lambda}\cdot(\vec{r}-\vec{r}')]}{\omega+i(\omega_\lambda+v\omega^0_{K-\lambda})} , \tag{3.5}$$

with ω_λ defined as $Jz(1-\gamma_\lambda)$, analogously to ω^0_λ in (2.10). For the case $\vec{r}=0$, Eq. (3.4) gives

$$f_K(0)=-xG_K , \tag{3.6}$$

as required since $\langle\langle p_l n_l;p_{g'}\rangle\rangle=0$. The equation for $\vec{r}=\vec{\delta}$ becomes, using (3.6) to eliminate $f_K(0)$,

$$\omega f_K(\delta)=iJ^0vxG_K[1-\exp(-i\vec{K}\cdot\vec{\delta})]-iz(J^0v+J)f_K(\vec{\delta})+i[J^0(v-x)+J]f_K(\vec{\delta})$$
$$+xJ^0f_K(-\vec{\delta})\exp(-i\vec{k}\cdot\vec{\delta})+i\sum_{\vec{\delta}'\neq\vec{\delta}}[J^0v\exp(-i\vec{K}\cdot\vec{\delta}')+J]f_K(\vec{\delta}-\vec{\delta}') , \tag{3.7}$$

which is conveniently written

$$f_K(\delta)=-i\sum_{\delta'}[1-\exp(-i\vec{K}\cdot\vec{\delta}')] \times T(\vec{\delta},\vec{\delta}')vxJ^0G_K , \tag{3.8}$$

where $\underline{T}$ is a matrix

$$\underline{T}=(\underline{1}-\underline{P}\,\underline{V})^{-1}\underline{P} , \tag{3.9}$$

confined to the $z+1$ sites $\vec{r}=\vec{0}$ or $\vec{\delta}$. $\underline{P}$ is given by (3.5) and $\underline{V}$ has the elements

$$V(\vec{\delta},\vec{\delta})=i[J^0(v-x)+J],$$
$$V(\vec{\delta},-\vec{\delta}')=iJ^0x\exp(-i\vec{K}\cdot\vec{\delta}) , \tag{3.10}$$
$$V(\vec{0},\vec{\delta})=-i[J^0v\exp(-i\vec{K}\cdot\vec{\delta})+J]$$
$$=V(-\vec{\delta},\vec{0}) ,$$

which represent the particle-vacancy interaction.

Combining Eqs. (3.2) and (3.8) the Green's function is

$$G_K=[\omega+i\Sigma(\vec{K},\omega)]^{-1} , \tag{3.11}$$

where the mass operator

$$\Sigma(\vec{K},\omega)=v\omega_K^0 F(\vec{K},\omega) \tag{3.12}$$

and

$$\omega_K^0 F(\vec{K},\omega)=\omega_K^0 + ix(J^0)^2\sum_{\vec{\delta}}\sum_{\vec{\delta}'}[1-\exp(i\vec{K}\cdot\vec{\delta})]T(\vec{\delta},\vec{\delta}')\times[1-\exp(-i\vec{K}\cdot\vec{\delta}')] . \tag{3.13}$$

Thus the approximation of decoupling in the second-order equation of motion yields a relatively simple closed-form expression for the mass operator which depends through T only on the parameters V, J, and J^0, and does not involve any self-consistency constraints of the type encountered in the coherent-potential approximation (CPA) theories[23] which we have applied to the specific case $J=0$ in the present problem.[24] For general $\vec{K}$ the matrix inversion required to obtain T is tedious and best performed numerically, but at points of high symmetry, relatively simple analytic expressions can be obtained.

Near $\vec{K}=0$, for example, $\Sigma(K,\omega)\sim iK^2D(\omega)$ and the coefficient D can be obtained from (3.13) by calculating T at $\vec{K}=0$ where it has full lattice symmetry, which has been taken to be cubic. In the long-wave length and small-frequency limit $K^2a^2 \ll \omega/J^0z \ll 1$ (where a represents the elementary cube edge in a Bravais cubic lattice) the correlation factor F reduces to the so-called diffusion correlation factor $f_0=F(\vec{K}\to\vec{0},\omega\to 0)$ and

$$G_K=\lim_{\substack{\vec{K}\to 0\\ \omega\to 0}}(\omega+ivf_0J^0K^2a^2)^{-1} . \tag{3.14}$$

Then, from (3.13),

$$f_0=\left[\frac{1}{6a^2}\right]\sum_{\vec{\delta}}\left[\delta^2+2xJ^0i\sum_{\vec{\delta}'}(\vec{\delta}\cdot\vec{\delta}')T(\vec{\delta},-\vec{\delta}')\right] . \tag{3.15}$$

For the simple cubic lattice (sc) this becomes

$$f_0=\{1+2xJ^0i[T(\vec{\delta},\vec{\delta})-T(\vec{\delta},-\vec{\delta})]\} . \tag{3.16}$$

The form of the second term in (3.16) is clearly related to the well-known lattice sum

$$\overline{\cos\theta}=\frac{1}{\delta^2}\sum_{\vec{\delta}}i(\vec{\delta}\cdot\vec{\delta}')P(\vec{\delta},\vec{\delta}') , \tag{3.17}$$

which is widely used to describe correlated diffusion[5,25] and is physically interpreted as the average cosine of the angle between successive jumps in a random walk. For cubic lattices,

$$\begin{aligned}\overline{\cos\theta}&=\left[\frac{1}{6N}\right]\sum_{\lambda}(C_{4x}-1)/(1-\gamma_\lambda)=-0.209\,842 \quad \text{(for sc lattice)}\\ &=\left[\frac{1}{8N}\right]\sum_{\lambda}(C_{2x}+1)(C_{2y}C_{2z}-1)/(1-\gamma_\lambda)=-0.157\,948 \quad \text{(for bcc lattice)}\\ &=\left[\frac{1}{12N}\right]\sum_{\lambda}[2(C_{2x}-1)(C_yC_z+C_{2x}C_{2y}-1)]/(1-\gamma_\lambda)=-0.122\,680 \quad \text{(for fcc lattice)} .\end{aligned} \tag{3.18}$$

Since f_0 only involves the p-wave part of $\underline{T}$ the full expression takes a relatively simple form to become after some manipulation,

$$f_0=\left[1-\frac{2J^0x\overline{\cos\theta}}{(J+J^0v)(1+\overline{\cos\theta})}\right]^{-1} . \tag{3.19}$$

This result is correct to first order in v, and first order in x, and generalizes the exact results known in the zero vacancy limit for a long time,[5] and for the small x limit obtained by us recently,[26,27] to the case $J\neq J^0$. The full extrapolated form (3.19) appears to be equivalent to the "multiple scattering approximation" of FS for $J=J^0$. [See Eq. (25), of Ref. 11 for f_0 in the sc lattice and Eqs. (22)–(24) of Ref. 14 for the fcc lattice.] For the sc case their result has the same form as (3.19) if the number -0.2118 is taken as $\overline{\cos\theta}$. For the fcc lattice the form of their result is different but numerically their value agrees with ours to within 0.5%. The extrapolated form also agrees with the computer simulation and Monte Carlo estimates within the accuracy of the latter (see Fig. 1).

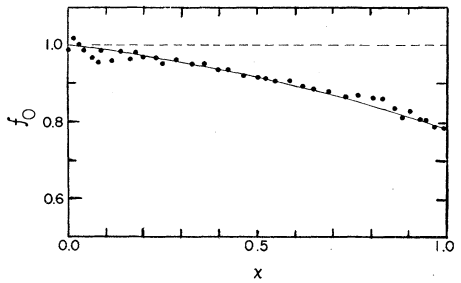

FIG. 1. Correlation factor f_0 predicted by Eq. (3.11) is given as a solid line for the fcc lattice with $J^0=J$. Closed circles represent the Monte Carlo simulation estimates of Kehr *et al.* (Ref. 18). Dashed line at top gives the MFA estimate.

A second point with a straightforward analytic solution is $\vec{K}a=(\pi,\pi,\pi)$ in the simple cubic lattice where the group of $\vec{K}$ is again the full cubic group. In this case $\exp(i\vec{K}\cdot\vec{\delta})=-1$ for all $\vec{\delta}$ and

$$P_K(\vec{r},\vec{r}')=\frac{1}{N}\sum_{\lambda}\frac{\exp[-i\lambda(\vec{r}-\vec{r}')]}{\omega+iz[J+vJ^0-(J-vJ^0)\gamma_\lambda]}\ . \tag{3.20}$$

The $\bar{T}$ matrix required for (3.13) now only involves s-wave scattering and after considerable manipulation we find

$$F(\vec{K},\omega)=\left[1+\frac{2xJ^0}{\left[iP_s^{-1}+\frac{4JJ^0v}{J+vJ^0}\right]}\right]^{-1}, \tag{3.21}$$

where

$$P_s=\frac{1}{N}\sum_{\lambda}\left[\frac{z\gamma_\lambda^2}{\omega+iz[J+vJ^0-(J-vJ^0)\gamma_\lambda]}\right]. \tag{3.22}$$

For the case $\omega=0$ we note anomalous behavior near $v=0$ where

$$P_s=\left[\frac{i}{J}\right]\left[0.5164+O\left[\frac{vJ^0}{J}\right]^{1/2}\right]. \tag{3.23}$$

These corrections of order $v^{1/2}$ are found at all zone-boundary points. The mass operator in this theory is correct to order v, but approximately treats processes involving vacancy pairs which are anticipated to be of order v^2. However, this calculation makes it clear that at the zone boundary there are corrections of order $v^{3/2}$ whose accuracy is uncertain.

For general hopping rates J of the background it is instructive to examine the behavior in two extreme limits. As $J/J^0\to\infty$ the background particles make many hops during the single hop of a tracer atom. The latter sees an average background and, as may be seen from (3.9) $T\to 0$ and $F(\vec{K},\omega)=1$, so that the mean-field approximation (MFA) result is recovered. The opposite limit $J=0$ corresponds to tracer hopping in a background of fixed blocked sites. As may be seen from (3.19) and (3.21) for specific cases, since $P(\vec{K},\omega)\propto v^{-1}$, $F(\vec{K},\omega)\propto v$ and this may be shown to be true in general using (3.8) and (3.9). Thus $\Sigma(\vec{K},\omega)$ varies as v^2 in our approximation. This is correct in the limit $v=0$, when no motion is possible, but incorrect to order v^2. For example, we know that diffusion is impossible, i.e., $f_0=0$ at $v<v_c$ the percolation limit, a result which is not reproduced by our theory. For this limiting case the CPA method developed earlier is more satisfactory.[24]

IV. NUMERICAL RESULTS

Although the analytic results of the preceding section are instructive, the general correlation parameter $F(\vec{K},\omega)$ contains a wealth of additional information. Owing to the importance of the small frequency regime, it is useful first to examine the properties of $F(\vec{K},0)$ as a function of both the wave-vector and the system concentration. For simplicity, we begin with the case $J^0=J$.

In Fig. 2 $F(\vec{K},0)$ is plotted as a function of $\vec{K}$ for the three directions $\vec{K}b/\pi=(k,0,0)$, $(k,k,0)$, and (k,k,k). For convenience, the abscissas are given in terms of the dimensionless variable k. Here $b=a$, for the simple cubic lattice [Fig. 2(a)], and $b=a/2$, for the fcc lattice [Fig. 2(b)]. The $\vec{K}$ dependence is found to be the most pronounced for a small vacancy concentration. [Results for five different vacancy concentrations, namely $v=0.0001$, 0.25, 0.5, 0.75, and 1.0, are recorded in Figs. 2(a) and 2(b)]. Another striking feature of these results is the total inversion of the $\vec{K}$ dependence that occurs somewhere between the concentrations $v=0.0001$ and $v=0.25$, contrasted with the seemingly slow and uneventful dependence on v for the $0.25<v<1$ regime.

In order to get a better understanding of the manner in which the inversion of the $\vec{K}$ dependence comes about as the vacancy concentration increases from 0.0001 to 0.25, in Figs. 3(a) and 3(b) the correlation parameter $F(\vec{K},0)$ is plotted as a function of the concentration x. Here the relevant $\vec{K}$ value for curves labeled 1 is (0,0,0); for curves 2 and 3 $\vec{K}b=(\pi/2,0,0)$ and $(\pi,0,0)$, respectively. As before, Figs. 3(a) and 3(b) are for the sc and the fcc lattices. Only for the sc lattice are there more than three curves shown. Here curves 4 and 5 are for $\vec{K}a=(\pi,\pi,0)$ and (π,π,π), respectively.

It is observed that for $v\to 0$, $F(\vec{K},0)$ undergoes rapid variation for $\vec{K}$ near the zone edge, as expected from the term in $v^{1/2}$ discussed in the preceding section. While the rate of change of $F(\vec{K},0)$ (with vacancy concentration) is slow and undramatic when $Kb\ll\pi$ [here one is basically dealing with $F(\vec{K},0)\sim f_0$], it is precipitous at the zone edge. Accordingly, for only a few percent vacancy concentration, the relative ordering of $F(\vec{K},0)$ for different wave vectors undergoes an inversion. As v increases beyond the inversion region, in these figures the concentration dependence of the correlation factor appears to show little qualitative change. The vacancy concentration at which the inversion occurs seems to depend upon the coordination of the lattice and is approximately twice as large for the fcc lattice as it

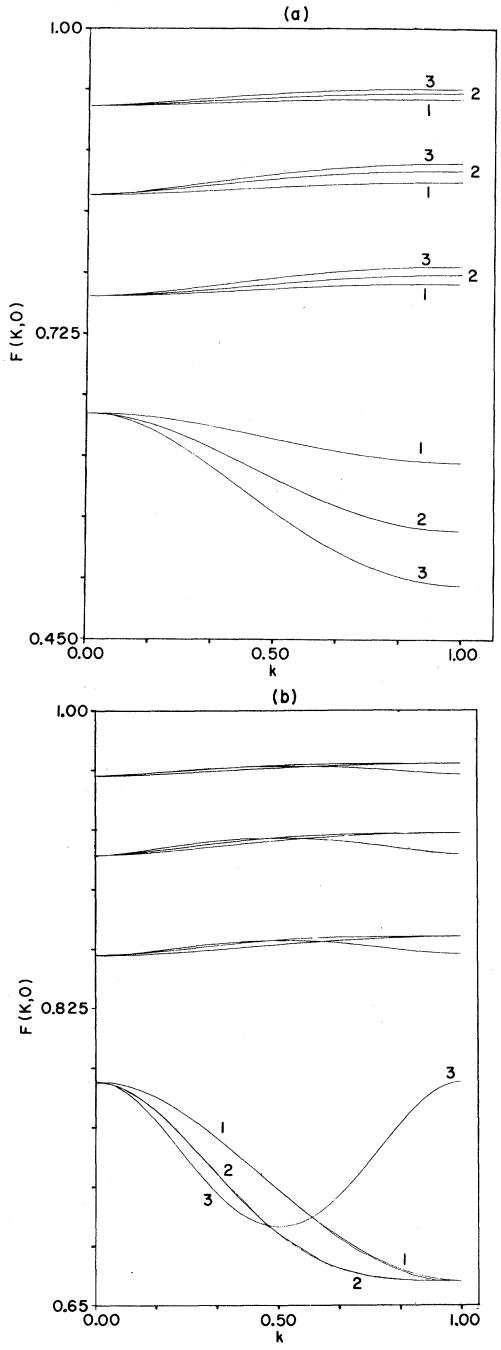

FIG. 2. For $J^0=J$, the generalized diffusion correlation factor for zero frequency $F(\vec{K},0)$ is plotted as a function of $\vec{K}$. Curves 1, 2, and 3 are for $\vec{K}b/\pi=(k,0,0)$, $(k,k,0)$ and (k,k,k), respectively. (a) Normalization parameter $b=a$ for the sc lattice and (b) $b=a/2$ for the fcc lattice. The bottom set of curves are for $v=0.0001$, while other sets, in the order of increasing heights, are for $v=0.25$, 0.5, and 0.75, respectively. Note that for $v=0.0001$ the order of curves 1, 2, and 3 is reverse of what it is for higher vacancy concentrations shown; also that for $v=1$, $F(\vec{K},\omega)=1$ for all $(\vec{K},\omega)$.

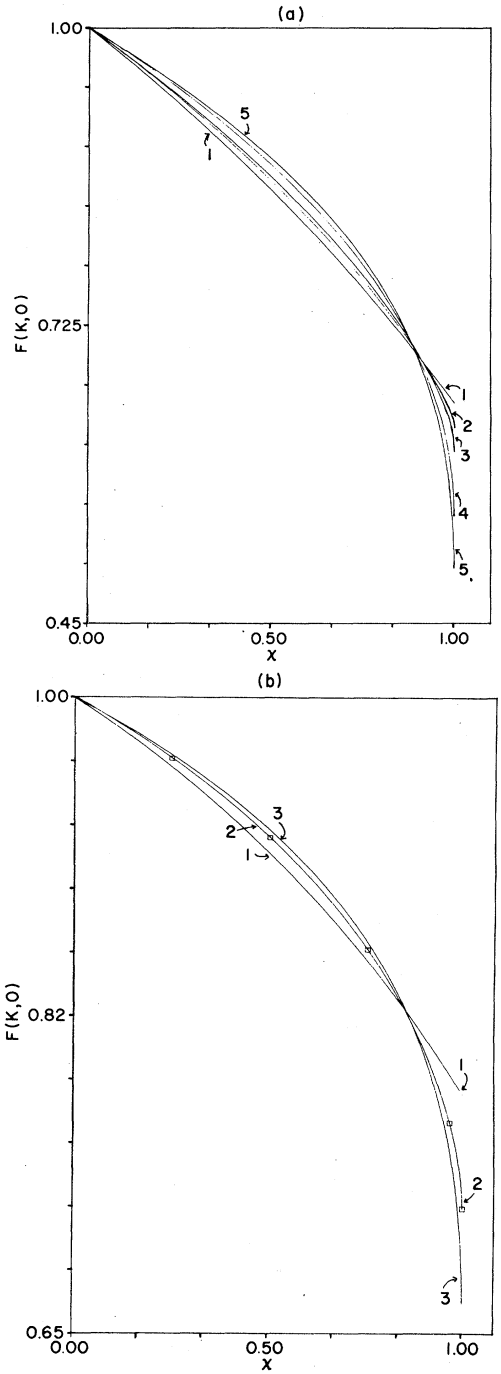

FIG. 3. $F(\vec{K},0)$ is given as a function of the concentration x. For curves 1, 2, and 3 $\vec{K}b=(0,0,0)$, $(\pi/2,0,0)$, and $(\pi,0,0)$, respectively. (a) refers to the sc lattice and (b) to the fcc lattice. For the sc case, curves 4 and 5 refer to $\vec{K}a=(\pi,\pi,0)$ and (π,π,π), respectively.

is for the sc.

This rapid variation of the mass operator for small vacancy concentration was partly foreseen in our previous work dealing with the $v=0$ limit.[6] Its

precipitousness was, however, somewhat underestimated when we used the mass operator, calculated for the $v=0$ limit, to compute the response function $S(\vec{K},\omega)$, for the case $v=0.012$ in the fcc lattice,

$$S(\vec{K},\omega)=\lim_{\epsilon\to 0+}-\frac{1}{\pi}\mathrm{Im}G_K(\omega+i\epsilon)\ . \tag{4.1}$$

[For practical reasons, all of the computations being reported in this paper were carried out with $\epsilon=10^{-5}(J^0z)$.] In view of the rapid variation with v at the zone edge, the $v=0$ result for the mass operator turns out to be approximately 10—15% of an underestimate for the case of $v=0.012$ in the fcc lattice. This results in a corresponding overestimate in the value of the response function. Consequently, our remarks based on the $v=0$ limit solution presented in an earlier paper,[6] about a possible underestimate in the Monte Carlo work of Kehr *et al.*[18] for the $\vec{K}b=(\pi,0,0)$ response in the fcc lattice were themselves an overstatement. Indeed, using the present theory we have recalculated the relevant response and find it to be in complete agreement with the Monte Carlo results of Kehr and others. (See Fig. 4.)

Despite the rather direct physical relevance of the response $S(\vec{K},\omega)$ the mass operator is a more convenient quantity to analyze for assessing the strengths and weaknesses of the theory. The reason for this convenience lies in the fact that while in the $\omega=0$ limit the response $S(\vec{K},\omega)$ directly measures the mass operator, or equivalently the correlation parameter $F(\vec{K},\omega)$, away from the low-frequency region the presence of the rapidly increasing quantity ω^2 in the denominator for $S(\vec{K},\omega)$—as can be seen from Eqs. (3.11) and (4.1)—effectively masks many of the variations occurring in the mass operator.

Accordingly, continuing the analysis of the $J^0=J$ case, in Figs. 5 and 6 we display the real and the (negative of the) imaginary parts of the generalized correlation factor $F(\vec{K},\omega)$ as a function of $\log_{10}(\omega/J^0z)$. It is clearly observed that the frequency dependence of $F(\vec{K},\omega)$ is qualitatively similar over a wide range of concentration. The exception to this rule would appear to arise in the small vacancy and large-$\vec{K}$ vector limits. In particular, for $v\to 0$ (rather than showing a mathematical limiting

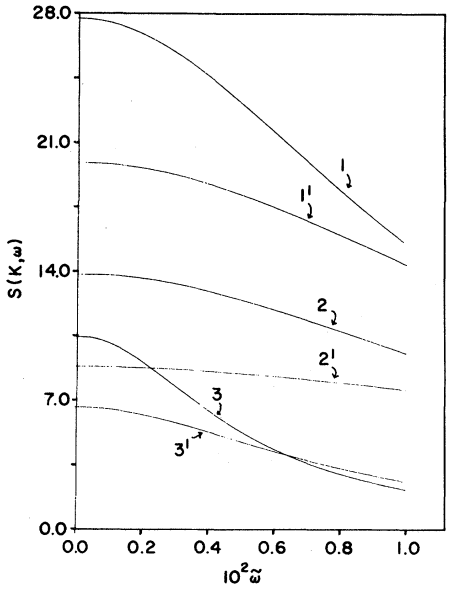

FIG. 4. Response $S(\vec{K},\omega)$ for $\vec{K}b=(\pi,0,0)$, $J^0=J$, and $v=0.012$ is given as a function of $(10^2\tilde{\omega})$ where $(\tilde{\omega}=\omega/J^0z)$. Curves 1, 2, and 3 refer to the fcc, bcc, and the sc lattices, respectively; curves 1′, 2′, and 3′ show the corresponding results obtained within the MFA. For convenience of display, for the bcc lattice (i.e., curves 2 and 2′) the plot shows $\frac{2}{3}S(\vec{K},\omega)$ whereas for the sc lattice (curves 3 and 3′) $S(\vec{K},\omega)/6$ is plotted.

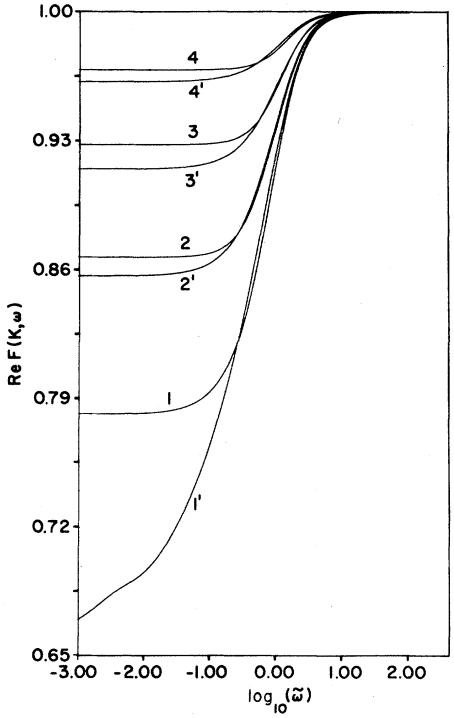

FIG. 5. For $J^0=J$ in an fcc lattice, $\mathrm{Re}F(\vec{K},\omega)$ is plotted as a function of $\log_{10}(\tilde{\omega})$ for wave vectors at the center and the edge of the Brillouin zone. We have chosen five different vacancy concentrations, i.e., $v=0.0001$ (curves 1,1′), $v=0.25$ (curves 2,2′), $v=0.50$ (curves 3,3′), $v=0.75$ (curves 4,4′), and $v=1$ (straight line at top). The $\vec{K}$ vector relevant to curves with unprimed labels is $\vec{K}=(0,0,0)$. For the curves with primed labels, $\vec{K}b=(\pi,0,0)$.

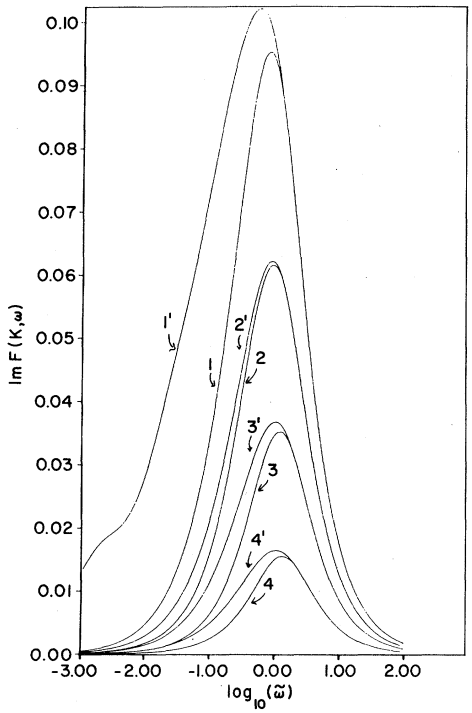

FIG. 6. Same as Fig. 5 with the difference that the function being plotted here is $-\mathrm{Im}F(\vec{K},\omega)$. Because the order of the curves is exactly inverted in this figure, as compared to the corresponding ones in Fig. 5, here the $v=1$ curve is represented by the straight line at the bottom showing $-\mathrm{Im}F(\vec{K},\omega)=0$.

case with $v=0$, we have chosen $v=0.0001$ as being more typical of the accessible physical limit), and $\vec{K}$ at the zone boundary, a gentle shoulder is observed as ω increases from about $10^{-4}J^0z$ toward $10^{-2}J^0z$. The shoulder moves closer to the higher-frequency end, i.e., $\sim 10^{-2}J^0z$, and at the same time its prominence decreases as z becomes larger.

For general hopping rates, in view of space limitations it is necessary to restrict the presentation of the data only to the more interesting physical limits. The small vacancy and small x limits would appear to fit this requirement best.

In Figs. 7(a)—7(c), the zero-frequency generalized correlation factor $F(\vec{K},0)$ is displayed for $v=0.0001$. No major qualitative changes in the spectrum are observed as the ratio J/J^0 changes. Of course as $J/J^0\to\infty$, $F(\vec{K},\omega)$ approaches 1 for all $\vec{K}$ and ω since the MFA becomes exact in this limit. Similarly, in the opposite limit, i.e., $J/J^0\to 0$, $F(\vec{K},\omega)$ becomes vanishingly small because the background is now completely static and the tracer can hardly move within it due to the paucity of vacant sites.

To display the frequency dependence of $F(\vec{K},\omega)$, it is convenient to work in terms of a composite, dimensionless frequency scale. For this purpose, a parameter Ω is introduced such that

$$\Omega=\begin{cases}\tilde{\omega} & \text{for } \tilde{\omega}\le 1\\ 1+\log_{10}(\tilde{\omega}) & \text{for } \tilde{\omega}\ge 1,\end{cases} \tag{4.2}$$

where $\tilde{\omega}=\omega/J^0z$. On this scale, the physically most interesting frequency regime, i.e., $0\le\tilde{\omega}\le 1$, is conveniently displayed linearly while on the same plot the steady approach to the MFA limit as $\tilde{\omega}\gg 1$ can also be accommodated.

These features of the generalized correlation factor $F(\vec{K},\omega)$ are presented for $v=0.0001$ in Fig. 8, where we show $\mathrm{Re}[F(\vec{K},\omega)]$, and in Fig. 9, where $-\mathrm{Im}[F(\vec{K},\omega)]$ is shown as a function of Ω. (For brevity, only the fcc results are shown here.) The interesting fact to observe here is the relative insignificance of the gentle, low-frequency shoulder when results for small frequencies are displayed on a linear, instead of a dilated logarithmic scale (compare and contrast this with Figs. 5 and 6).

For general concentrations, space limitations dictate the study of the relatively more interesting zero-frequency properties. Because the bcc lattice results are approximately intermediate between those for sc and fcc lattices, in Fig. 10 the correlation factor $F(\vec{K},0)$ for the bcc lattice is plotted as a function of the concentration x. [Note $F(\vec{K},0)$ is real for all K vectors in the zone.] Here the top set of two curves, labeled 1 and 1′, refer to $J/J^0=5$, the middle set (labeled 2,2′) to $J/J^0=1$, and the lowest set (labeled 3,3′) to $J/J^0=\frac{1}{5}$. Curves 1, 2, and 3 refer to $\vec{K}=\vec{0}$, whereas curves 1′, 2′, and 3′ refer to $\vec{K}b=(\pi,0,0)$.

The major effect of increasing the ratio J/J^0 is seen to be the shifting of the crossover away from the low-vacancy region. Moreover, the three cubic lattices differ in two regards. Firstly, the crossover moves closer to the $v\to 0$ end as z decreases from 12 to 6 and, secondly, the separation in the two curves (referring to the same ratio J/J^0) increases, i.e., the $\vec{K}$ dependence becomes stronger as z changes from 12 to 6.

For the small concentration region, i.e., $x\ll 1$, all the various curves in Fig. 10 appear to behave similarly. This is, largely speaking, an optical illusion because on the scale plotted it is hard to make out the differences in the slopes at $x=0$. To bring this feature out, it is convenient to analyze $\alpha(\vec{K},\omega)$ where

$$F(\vec{K},\omega)\underset{x\ll 1}{=}1-x\alpha(\vec{K},\omega)+O(x^2)\,. \tag{4.3}$$

It should be recalled that the present theory leads to an exact expression for $\alpha(\vec{K},\omega)$ for all ratios J/J^0.

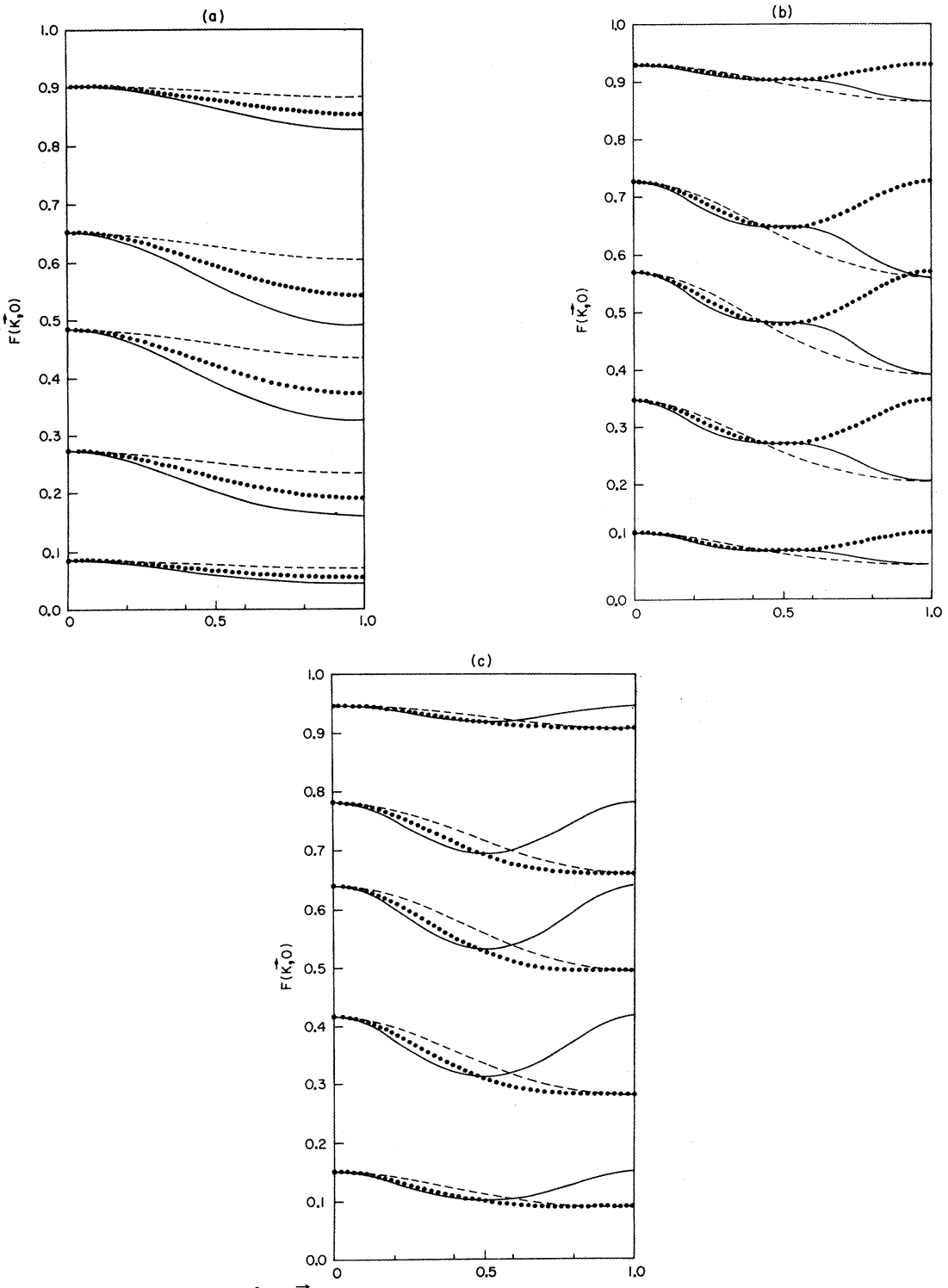

FIG. 7. For different ratios of J/J^0, $F(\vec{K},0)$ is plotted for $v=0.0001$ as a function of k. The continuous curves refer to $\vec{K}b/\pi=(k,k,k)$ while the dotted and the dashed curves are for $\vec{K}b/\pi=(k,k,0)$ and $(k,0,0)$, respectively. In units of $J^0z=1$, $Jz=5$ for the top set of three curves, 1 for the next lower set, $\frac{1}{2}$ for the middle set, $\frac{1}{5}$ for the set of curves above the lowest one, while $Jz=\frac{1}{20}$ for the lowest set of three curves. The relevant lattices are (a) sc, (b) bcc, and (c) fcc. Note $F(\vec{K},0)$ approaches the top or the bottom straight lines as $Jz\to\infty$ or $Jz\to 0$. The former case corresponds to the mean-field limit, whereas the latter refers to the case of a tracer diffusing against a background of static particles.

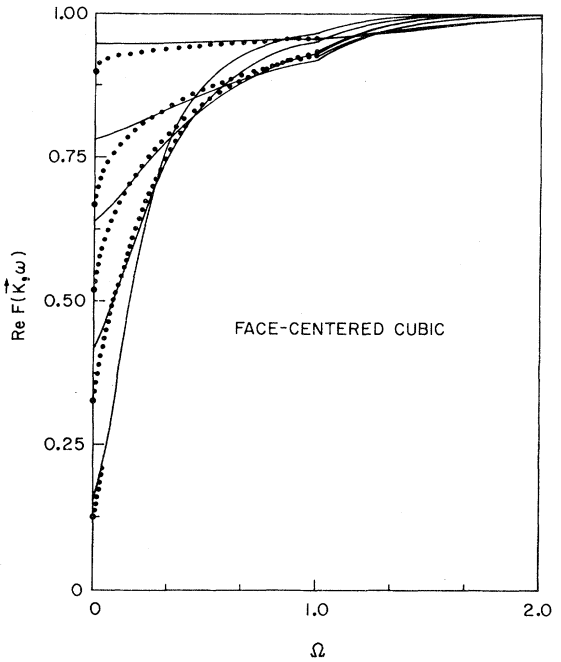

FIG. 8. For $v=0.0001$ and $J^0z=1$, the real part of $F(\vec{K},\omega)$ is plotted as a function of Ω. Beginning with the top set of two curves (the higher being continuous and the lower one dotted) and coming down the zero-frequency axis, the relevant values of Jz for various sets are the following: 5, 1, $\frac{1}{2}$, $\frac{1}{5}$, and $\frac{1}{20}$. The continuous curves refer to $\vec{K}=(0,0,0)$. For the dotted curves $\vec{K}b=(\pi,0,0)$.

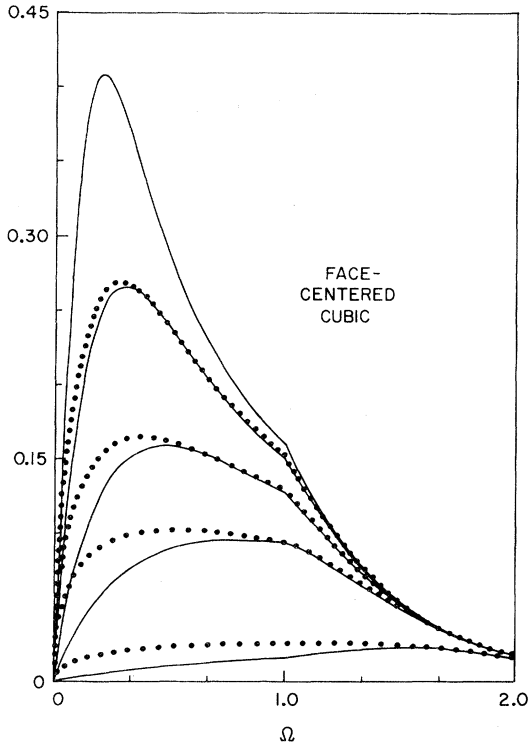

FIG. 9. Same as Fig. 8 with the difference that here the function being plotted is $-\mathrm{Im}F(\vec{K},\omega)$ and the ordering in relative heights of the curves is exactly inverted. Note also that the top continuous curve in this figure represents the set of curves for $Jz=\frac{1}{20}$ and that the shown thickness of this curve accommodates all the $\vec{K}$ values within the Brillouin zone.

Again, the most interesting feature of $\alpha(\vec{K},\omega)$ appears to be its wave-vector dependence at $\omega=0$. To bring this out, in Figs. 11(a)—11(c) $\alpha(\vec{K},0)$ is plotted as a function of $\vec{K}$.

A dramatic dependence on $\vec{K}$ is observed for $J/J^0=0$ (see the top set of three curves in each of these figures). Somewhere within the regime $0\leq J/J^0\leq\frac{1}{3}$, the relative ordering of the curves undergoes an inversion and thereafter the behavior of the curves does not undergo any qualitative change [except for the fact that as J/J^0 increases, the MFA become progressively more accurate and $\alpha(\vec{K},\omega)$ moves toward zero].

V. CONCLUSION

In order to best set the results of this paper into their proper perspective, two aspects of the theory need special attention. First, is the exactness of the theory at the two concentration ends. A direct consequence of this fact is the exactness of the parameters $\alpha(\vec{K},\omega)$ in the limit $x\to 0$, and $F(\vec{K},\omega)$ in the limit $v\to 0$. In this regard, the feature of particular interest is the contrasting behavior of the $v=0$ and the $x=0$ results as a function of the ratio

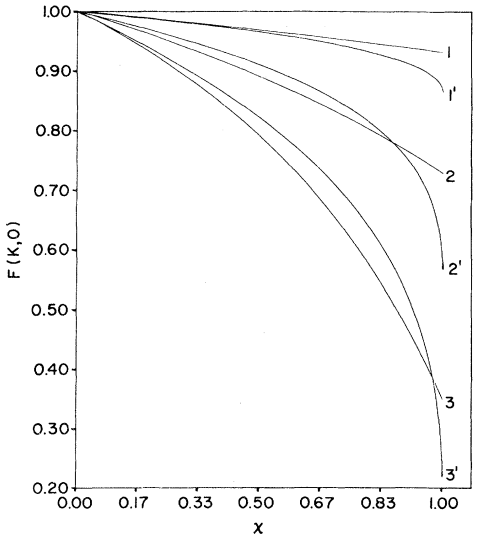

FIG. 10. For the bcc lattice, $F(\vec{K},0)$ is plotted in terms of concentration x. For curves 1, 2, and 3, $\vec{K}=0$. Curves 1′, 2′, and 3′ refer to $\vec{K}b=(\pi,0,0)$. The top set of two curves (1,1′) refers to $J/J^0=5$, the middle set (2,2′) to $J/J^0=1$, and the lowest set (3,3′) to $J/J^0=\frac{1}{5}$.

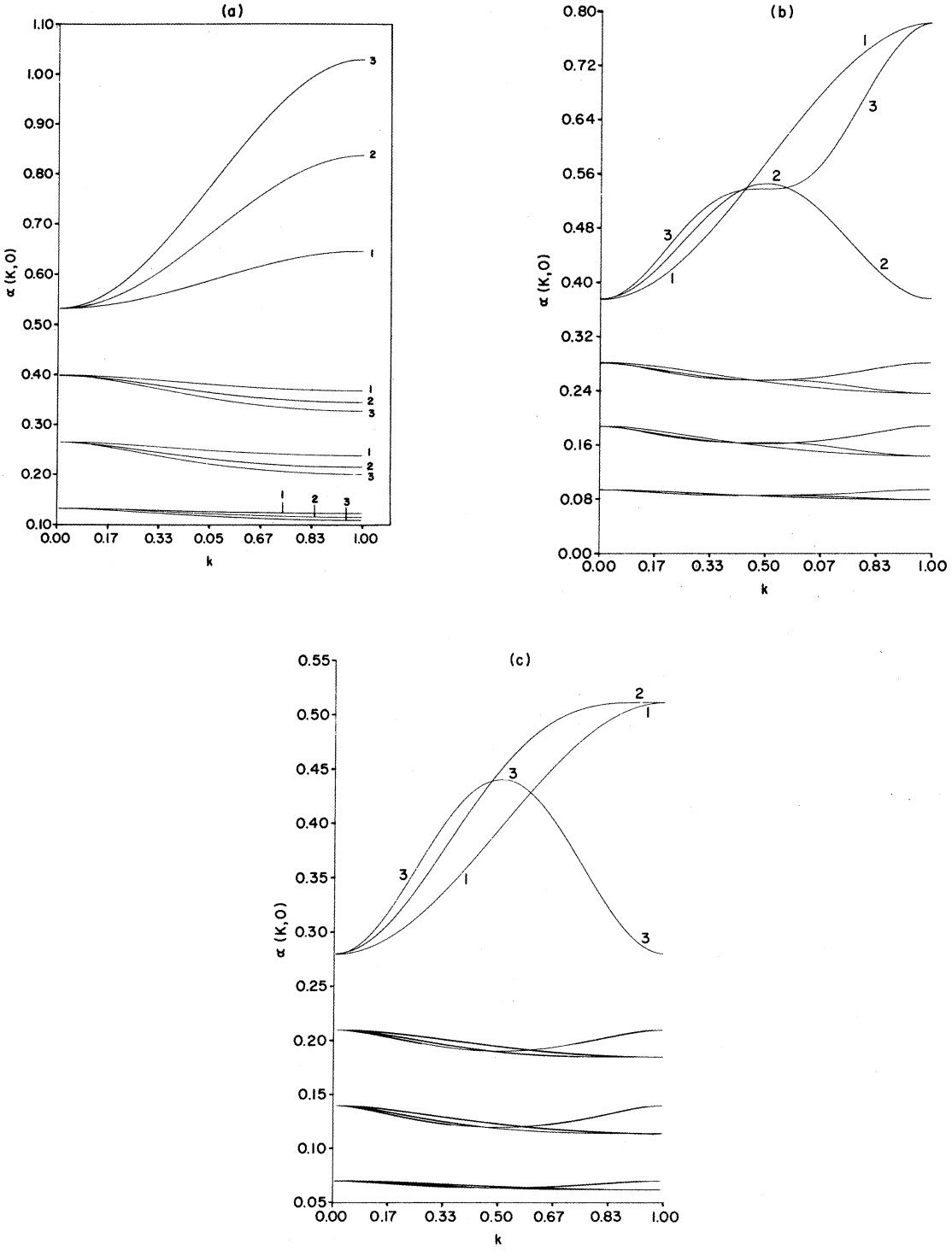

FIG. 11. $\alpha(\vec{K},0)$ is plotted as a function of k such that $\vec{K}b/\pi=(k,0,0)$, for curves labeled 1, whereas for curves 2 and 3 it is $=(k,k,0)$ and (k,k,k), respectively. The top set of three curves refers to $J/J^0=0$, the next lower set to $J/J^0=\frac{1}{3}$, the set above the lowest is for $J/J^0=1$, while the lowest set pertains to $J/J^0=3$. Relevant labeling is recorded on all the curves only in (a) (the sc lattice). In (b) (bcc lattice) and (c), it is convenient to label only the top set of three curves and to note that as in (a), for all the lower sets the ordering of the curves is exactly inverted.

J/J^0. For given $\vec{K}$ and ω, while the results for $F(\vec{K},\omega)$ at $v=0$ are all qualitatively similar (as a function of J/J^0), this is manifestly not the case at the $x=0$ end. Here the parameter $\alpha(\vec{K},\omega)$ undergoes a gradual but, nonetheless, dramatic inversion of its $\vec{K}$-dependent characteristics as the ratio J/J^0 is increased from zero through some critical value ρ_c toward infinity.

The second noteworthy aspect of the theory refers to the inversion of the $\vec{K}$-dependent characteristics of the generalized correlation factor $F(\vec{K},\omega)$ as the concentration is varied between the two ends. The details of this latter inversion are also observed to be strongly dependent upon the ratio J/J^0, indicating both a relationship of the two inversion processes and also pointing out possible inadequacies in the theory in the intermediate concentration range when the ratio J/J^0 is decreased from large values toward zero.

Before proceeding further, it is instructive to examine the magnitude of what has been referred to as the critical ratio of J/J^0 ρ_c. For the simple cubic lattice, which is the most non-mean-field-like lattice of the three Bravais cubic lattices, we have computed ρ_c to be $\sim 0.120 \pm 0.002$ (for bcc and the fcc lattices ρ_c would be somewhat smaller). Thus, for the cubic lattices, the large fluctuation effects associated with the crossover from one type of qualitative behavior to another occur when J is of order $J^0/6$ or smaller. Consequently, in three dimensions the present approximation scheme can be expected to get progressively more meaningful as the ratio J/J^0 increases beyond about $\frac{1}{6}$. Indeed, for large ratios J/J^0, even the unembellished MFA would become accurate.

In view of the above, a rough estimate for the region of adequacy (over the entire concentration range) of the present theory would be $J/J^0 \gtrsim \frac{1}{5}$. However, in lower dimensionality, we expect this requirement to become considerably more stringent. Accordingly, even for $J/J^0 \sim 1$, improvements over the second-order theory presented here would be needed so as to adequately describe lower-dimensional systems.

(Note to the readers: Owing to space limitations, only a small fraction of the computed results have been presented. Readers who are interested in additional results are encouraged to contact the authors.)

ACKNOWLEDGMENTS

This work was begun in Oxford with the support of the National Science and Engineering Research Council. It was continued while one of us (R.A.T.-K.) was in Kyoto and he is indebted to Professor T. Kawasaki for hospitality and to the Kyoto University 70th Anniversary Fund for support. He would also like to acknowledge that, in addition, his work was supported in part by National Science Foundation Grant No. DMR-8013700 and a Temple University Grant-in-Aid. Another of us (R.J.E.) is indebted to Florida State University where part of the work was carried out. Helpful discussions with Professor Y. Nagaoka, Professor Y. Kuramoto, Professor K. Tomita, Professor T. Kawasaki, Professor T. Holstein, Professor D. K. Ross, Professor K. Singwi, and Professor Yung-Li Wang are gratefully acknowledged. Dr. Kehr's kindness in communicating and explaining the Monte Carlo results as this paper was being written has been much appreciated.

[1]For a recent review, see *Physics of Superionic Conductors,* Vol. 15 of *Topics in Current Physics,* edited by M. B. Salamon (Springer, New York, 1979).

[2]For a comprehensive review of the relevant literature before 1970, see A. D. LeClaire, in *Physical Chemistry,* edited by W. Jost (Academic, New York, 1970), Vol. 10.

[3]See, for example, T. Springer, in Vol. 3 of *Topics in Current Physics,* edited by M. Lovesey and T. Springer (Springer, New York 1977). Also, *Diffusion in Solids—Recent Developments,* edited by A. S. Norwick and J. J. Burton (Academic, New York 1975).

[4]J. Bardeen and C. Herring, in *Imperfections in Nearly Perfect Crystals,* edited by W. Shockley (Wiley, New York, 1952).

[5]A. D. LeClaire and A. B. Lidiard, Philos. Mag. 1, 518 (1956).

[6]R. A. Tahir-Kheli and R. J. Elliot, J. Phys. C 15, L445 (1982).

[7]H. C. Torrey, Phys. Rev. 92, 262 (1953).

[8]K. S. Singwi and A. Sjölander, Phys. Rev. 119, 863 (1960).

[9]C. J. Chudley and R. J. Elliott, Proc. Phys. Soc. London 77, 33 (1961).

[10]P. A. Fedders and O. F. Sankey, Phys. Rev. B 15, 3580 (1977).

[11]P. A. Fedders and O. F. Sankey, Phys. Rev. B 18, 5938 (1978).

[12]P. A. Fedders, Phys. Rev. B 18, 1055 (1978).

[13]O. F. Sankey and P. A. Fedders, Phys. Rev. B 15, 3586 (1977).

[14]O. F. Sankey and P. A. Fedders, Phys. Rev. B 20, 39 (1979).

[15]O. F. Sankey and P. A. Fedders, Phys. Rev. B 22, 5135

(1980).

[16]Note, however, that Sankey has provided an explicit result for the $\omega \to 0$, $v \to 0$, $\vec{K}$-dependent mass operator for the simple cubic lattice in the form of a curve. Judging from this curve, the Fedders-Sankey results for the $\omega \to 0$, $v \to 0$ limit are substantially in error near the zone edge. [Compare O. F. Sankey, Ph.D. thesis, Graduate School of Arts and Sciences, Washington University, St. Louis, Missouri, 1969 (unpublished), Fig. 8(a), and the results for $v \to 0$ reported in Ref. 6].

[17]H. J. DeBruin and G. E. Murch, Philos. Mag. 27, 1475 (1973).

[18]K. W. Kehr, R. Kutner, and K. Binder, Phys. Rev. B 23, 4931 (1981).

[19]Compare, for instance, K. W. Kehr, in *Proceedings of the International Symposium on the Electronic Structure and Properties of Hydrogen in Metals, Richmond, Virginia, 1982,* edited by P. Jena (Plenum, New York, 1983).

[20]K. W. Kehr, R. Kutner, and K. Binder (unpublished).

[21]K. W. Kehr (private communication).

[22]P. M. Richards, Phys. Rev. B 16, 1393 (1977).

[23]R. J. Elliott, J. Krumhansl, and P. L. Leath, Rev. Mod. Phys. 46, 465 (1974).

[24]K. K. Kaski, R. A. Tahir-Kheli, and R. J. Elliott, J. Phys. C 15, 209 (1982).

[25]C. A. Sholl, J. Phys. C 14, 2723 (1981).

[26]R. A. Tahir Kheli, R. J. Elliott, and K. K. Kaski, Phys. Lett. 88A, 473 (1982).

[27]R. A. Tahir-Kheli and R. J. Elliott, J. Phys. C 15, 5751 (1982).